JOURNAL OF CATALYSIS 86, 373–383 (1984)

Oxidation of Carbon Monoxide on Thin Film Catalysts: Characterization by a Critical Temperature Measurement

J.-P. DAUCHOT AND J.-P. DATH[1]

Service de Chimie Analytique et Inorganique, Faculté des Sciences, Université de l'Etat à Mons, Avenue Maistriau 23, 7000 Mons, Belgium

Received April 14, 1982; revised May 31, 1983

Platinum catalyst thin films prepared by PtO_2 decomposition are tentatively characterized by the transition between two stationary reaction states both at constant temperature and constant CO partial pressure. It is demonstrated that at constant temperature, the measurements must be made in the sense of decreasing CO concentration because of reactant diffusion and heat dissipation. Following the model of R. Dagonnier, M. Dumont, and J. Nuyts (*J. Catal.* **66,** 130 (1980)), a sum of activation energies corresponding to the surface reaction and the dissociative oxygen adsorption was determined. This sum of activation energies and the ordinate axis intercepts of the Arrhenius plot presented are found to change with ageing of the samples.

INTRODUCTION

Carbon monoxide oxidation on platinum has been studied in various experimental conditions and it is rather clearly established now that the reaction mechanism is of Langmuir–Hinshelwood type (*1–3*). In this condition, it has been demonstrated (*4*) that a critical temperature (T_C) exists under which the reaction cannot occur or a critical ratio $[CO]/[O_2]$ (denoted hereafter as $[CO]^*$) beyond which the reaction stops. Thus the kinetic behavior at constant temperature is the following: the reaction rate rises with the $[CO]/[O_2]$ ratio in the gas phase and falls abruptly when it reaches this critical ratio (Fig. 1). On the other hand, at constant $[CO]/[O_2]$, the reaction rate remains near zero as long as the temperature has not reached the critical value T_C, at which it suddenly becomes very high.

In the active region, the surface is oxygen-covered; the oxygen coverage is close to unity and the CO coverage near zero. This fact was observed by Dauchot and Van Cakenberghe (*5*) at atmospheric pressure and by Matsushima *et al.* (*2*) and Golchet and White (*3*) at very low pressure. The reverse situation, namely CO coverage near unity and oxygen coverage near zero, is obtained beyond the inhibition ratio (or below the critical temperature). It should be noted that at low pressure (*2, 3*) a reaction with negative order in CO after the transition is observed. In our conditions (atmospheric pressure and $300\ K < T < 473\ K$) the reaction rate is very low but can be observed by working with very large surface catalysts (Fig. 2).

In the model proposed by Dagonnier, Dumont, and Nuyts (DDN) (*4*) the transition point (T_C or $[CO]^*$) is related to the sum of the activation energies of the oxygen adsorption and of the surface reaction between adsorbed carbon monoxide and oxygen.

The aim of our work has been to study this critical point at atmospheric pressure and between 30 and 160°C in order to characterize the catalytic surfaces by seeing how this sum of activation energies varies as a function of different parameters, e.g., preparation and ageing.

The DDN model (*4*) is based on the following assumptions.

[1] I.R.S.I.A. specialization fellowship.

0021-9517/84 $3.00

1. CO and O_2 are adsorbed competitively on the same sites.

2. The reaction rate can be described as a function of the CO and oxygen coverages (O_2 is adsorbed dissociatively).

3. The reaction proceeds only by an activated Langmuir–Hinshelwood (LH) mechanism between dissociatively adsorbed oxygen and adsorbed carbon monoxide. The CO_2 does not stay on the surface because of its low adsorption heat.

4. The adsorption of oxygen has second-order kinetics on the free surface sites and is activated, whereas the adsorption of carbon monoxide has first-order kinetics and is not an activated process.

5. The reaction conditions are isothermal.

This model leads to the following expression for the critical temperature:

$$T_C = \frac{B_2'' + C''}{\ln \dfrac{C'\sigma_{O_2} \cdot N_S \cdot \sqrt{2\pi m_{O_2} k T_C}}{4 p_{O_2} \sigma_{CO}{}^2 \dfrac{m_{O_2}}{m_{CO}}} - 2\ln \dfrac{p_{CO}}{p_{O_2}}} \tag{1}$$

which may be written as

$$2\ln\left(\frac{p_{CO}}{p_{O_2}}\right) = -\frac{C'' + B_2''}{T_C} + \ln \frac{C'\sigma_{O_2} \cdot N_S \cdot \sqrt{2\pi m_{O_2} k T_C}}{4 p_{O_2} \sigma_{CO}{}^2 \dfrac{m_{O_2}}{m_{CO}}} \tag{2}$$

where C'' and B_2'' are, respectively, the activation energy of the surface reaction and of the oxygen adsorption divided by the gas constant R, and where C' is the preexponential factor of the surface reaction (LH) rate constant. σ_{O_2}, σ_{CO}, m_{O_2}, and m_{CO} are, respectively, the sticking coefficients of oxygen and carbon monoxide (exponential factor excluded) and their molecular weights; N_S is the number of sites per unit of area, k is the Boltzman constant.

The validity of the assumptions leading to these equations will be examined later in the discussion.

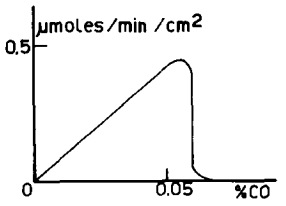

FIG. 1. CO_2 production versus CO partial pressure in the reactant mixture at 135°C.

EXPERIMENTAL

a. Sample Preparation

The samples are prepared as PtO_2 deposited on oxidized silicon wafers (0.5 μm of SiO_2) by dc reactive sputtering in an argon–oxygen mixture (*6*). They are stored in this form and decomposed to platinum just before the experiment. The platinum thicknesses are between 100 and 500 Å.

The samples used are of two different sizes. The first ones are squares of about 1 cm^2 and the second ones are small rectangular pieces (dots) of 100 μm × 2 mm size (Fig. 3). The electrical contacts and the siz-

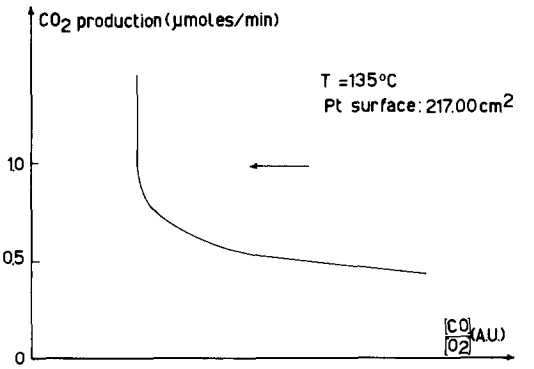

FIG. 2. CO_2 production in the "inhibited" region on a large surface Pt thin film. The curve is obtained by decreasing the CO concentration given by the opening level of the needle valve.

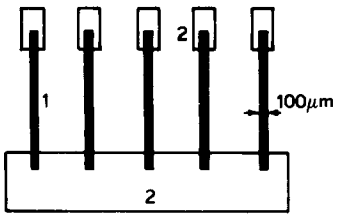

FIG. 3. Aspect of the small samples. (1) Platinum. (2) Gold contacts.

ing of the small platinum dots are made by photolithography.

b. Measurement Method

The critical point is obtained by detecting the change of reaction rate or of coverage at the transition.

The reaction rate is followed by measuring the CO_2 production as detected by infrared absorption at 4.5 μm. The oxygen flow is fixed at 250 cm^3/min and the CO concentration can be increased or decreased by a needle valve slowly opened or closed electrically which regulates the flow rate of a mixture of CO (0.5%) in nitrogen. A potentiometer placed on the axis of the valve gives a voltage proportional to the opening level and therefore a measure of the CO concentration (after calibration by ir absorption at 4.7 μm).

The coverage variations are detected by following the resistance of the film on the small platinum dots. Their resistivity varies about 10% when the coverage inversion occurs. This behavior can be interpreted by different theoretical models for the conductivity of thin metallic films (*7*, *8*) but in this work this property is only used to detect the coverage transition.

RESULTS

a. Constant-Temperature Measurements

In all the measurements, the total pressure in the cell may be considered as equal to the atmospheric pressure.

Both CO_2 production on a large sample (1 cm^2) and electrical resistance representative of the coverage on a small sample (100 μm × 2 mm) are followed simultaneously (the two samples are placed in the cell near each other) as a function of increasing and decreasing $[CO]/[O_2]$ ratio. The different curves obtained at a particular temperature are shown in Fig. 4 and Table 1 reproduces the results for various temperatures.

The main fact to be noticed is that in the sense of increasing [CO] the critical ratio [CO]* is higher on the large sample (by infrared detection) than on the small one (by resistance determination). In the sense of decreasing [CO], the two determinations are the same. It must be concluded that

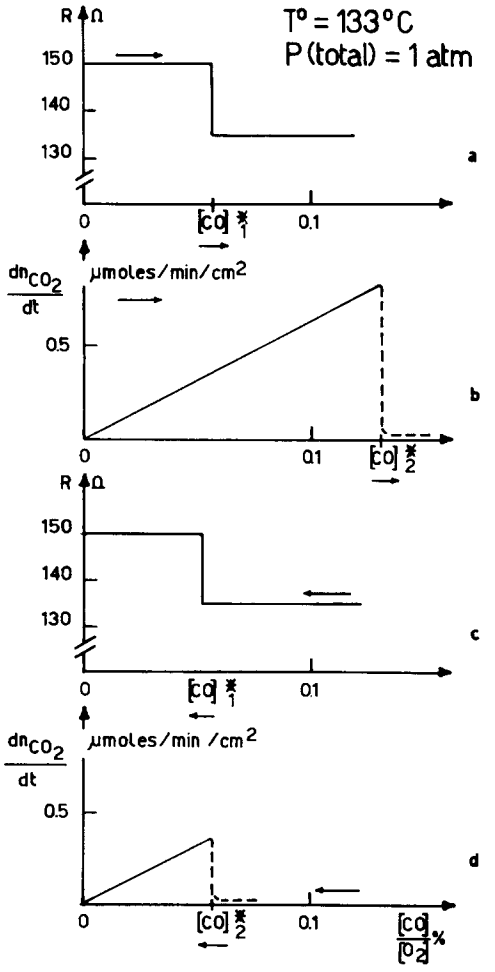

FIG. 4. Resistance and reaction rate versus CO partial pressure. (a) and (b): Increasing [CO] sense. (c) and (d): Decreasing [CO] sense.

TABLE 1

Critical Ratio [CO]* Values for the Small (1) and the Large (2) Samples when Increasing (a) and Decreasing (b) CO Concentration

T (°C)	$[CO]^*_{1a}$ (%)	$[CO]^*_{2a}$ (%)	$[CO]^*_{1b}$ (%)	$[CO]^*_{2b}$ (%)
133	0.057	0.131	0.052	0.057
124	0.050	0.114	0.048	0.048
117	0.046	0.095	0.044	0.044

[CO]* detected in the sense of increasing [CO] depends not only on the catalyst nature but also on geometrical factors. In the sense of increasing [CO] the catalyst is very active; the surface is heated by the reaction itself and the reaction becomes mass transfer limited. The temperature on the catalyst being higher than the bath temperature and [CO] near the surface being lower than in the gas phase, the [CO]* is displaced to larger values. These effects are greatly attenuated on small samples where the CO diffusion in the gas phase and heat dissipation have cylindrical symmetry and are therefore more efficient than in a planar symmetry as in the large sample. This interpretation accounts for the fact that in the sense of decreasing [CO], the [CO]* values determined on the two kinds of samples are identical. Indeed in this case the reaction before the transition is very slow and there is no effect of temperature or diffusion. Moreover, the lower the bath temperature, the lower is the difference between the two [CO]* values taken in the increasing [CO] sense (Table 1).

The conclusion of this kind of experiment is that the real [CO]* defined by Eqs. (1) and (2) must be detected by decreasing [CO] (for this reason, the recording of Fig. 2 was taken in a decreasing [CO] sense). Thus it has been measured in a range of temperature between 90 and 160°C. In this experiment [CO] has been followed by infrared absorption at 4.7 μm and the transition has been detected by the resistance variation. In Fig. 5, ln [CO]* is plotted versus $1/T$. From Eq. (2), a sum of activation energies of about 16 kcal/mole is found. (It must be noted that taking into account the variation of p_{O_2} and $\sqrt{T_C}$ in the last term of the right member of Eq. (2) does not modify the general aspect of this Arrhenius plot).

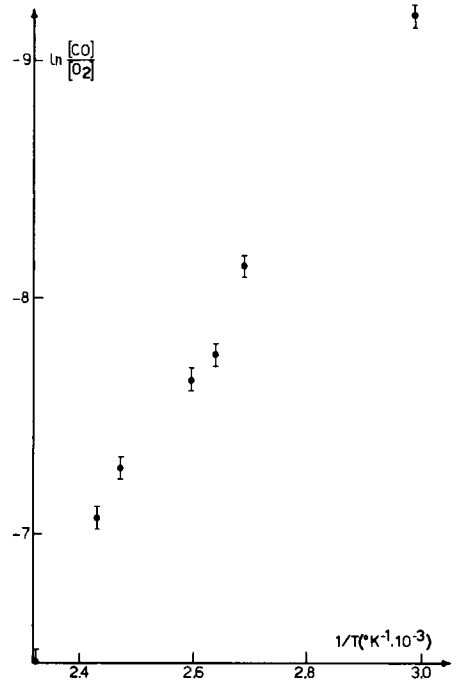

FIG. 5. Arrhenius plot of [CO]* determined at constant temperature versus $1/T$.

Unfortunately, due to the large error in the $[CO]/[O_2]$ infrared determination, this measure is not accurate enough to characterize a sample. Indeed, in order to have a fast response time, we must use a small optical path ir cell and at the low concentration which we have to measure, the relative error on $[CO]/[O_2]$ determined by ir is estimated to be 10%. For this reason, the second method of measurements we describe below was developed.

However, the comparison between small and larger samples when increasing or decreasing $[CO]/[O_2]$ proves the role of reactant diffusion and surface temperature of the sample. This is an important result for the realization of the critical temperature measurements.

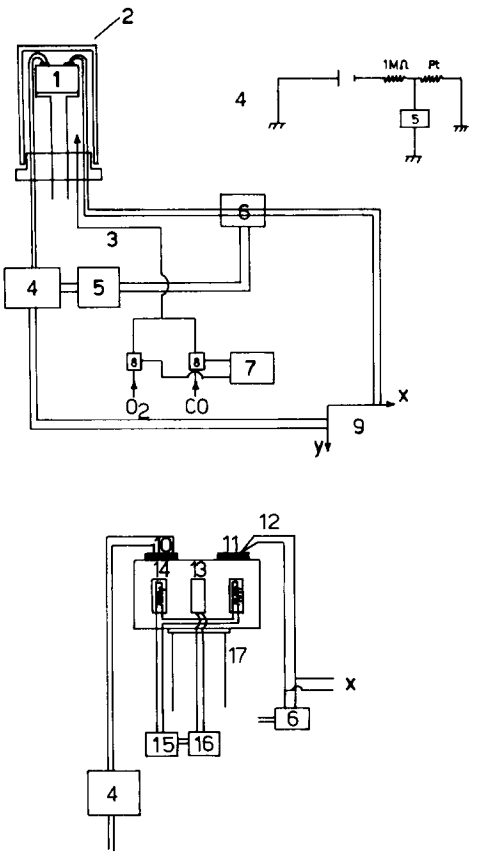

FIG. 6. Experimental setup for critical temperature measurement. (1) Thermostabilized gold-plated block; (2) Dewar vessel. (3) gas mixture arrival; (4) resistance measurement circuit; (5) amplifier; (6) digital voltmeter; (7) flowmeter; (8) regulated valves; (9) x–y recorder; (10) sample; (11) oxidized silicon; (12) thermocouple; (13) thermoresistance; (14) heater; (15) power supply; (16) thermal regulation.

b. Constant $[CO]/[O_2]$ Ratio Measurements

In order to avoid errors due to the nonuniformity of temperature it was decided to work on very small samples. This was made possible by detecting the transition on the small resistances (Fig. 3). The experimental setup is pictured in Fig. 6. Two Brooks thermal flowmeters control the $[CO]/[O_2]$ ratio. The total flow rate is not held constant but it was verified that a change of a factor of two in this quantity does not influence the measurements. The main parameter is then the ratio $[CO]/[O_2]$. By standardization we estimate the relative error on this ratio to be less than 0.5%. The sample is put on a heated gold-plated copper block placed in a small Dewar vessel. In order to have a good measurement of the critical temperature, a thermocouple is pasted with silver lake on an oxidized silicon chip identical to the sample substrate. It has been preliminarily verified by putting two thermocouples on two different chips in the same conditions that the difference between the sample temperature and the value given by the thermocouple cannot be more than 0.2°C.

The $[CO]/[O_2]$ ratio is fixed at a value where the reaction is inhibited. In these conditions, no effect of temperature on diffusion can influence the measurement. The temperature is slowly increased (5°C/min). At the transition the signal given by the resistance triggers a digital voltmeter which measures the voltage of the thermocouple placed near the sample.

Resistance measurements are affected by the platinum temperature but this variation is linear with T, while the change of resistance at the transition is very abrupt and it can be considered as an image of an abrupt change of coverage: it is parallel to the change of the platinum surface potential in the same conditions (see, for instance, the measurements in Ref. (*5*)).

The first observation was the change of T_C provoked by repeated cycling of the transition itself or by a period in oxygen atmosphere, as shown in Fig. 7 where T_C is plotted as a function of the transition number undergone by the sample. It must be noted that Fig. 7 illustrated just an example of change of T_C versus the measurement number. Indeed the change of T_C depends on the time the sample spends in the active phase after the transition has occurred, which is not easily controllable.

A treatment in pure CO at 160°C during 1 h was found to restore the critical temperature value of the first transition. Thus we have measured the critical temperature for

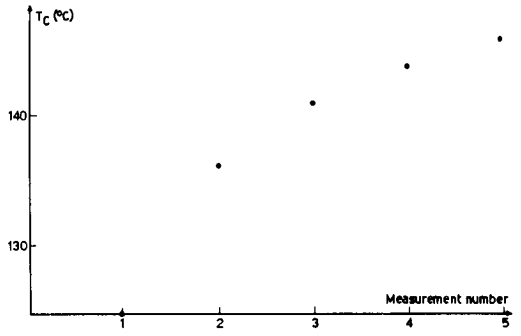

FIG. 7. Critical temperature versus the measurement number.

different $[CO]/[O_2]$ ratios with such a treatment between each measurement.

In Fig. 8, ln $[CO]/[O_2]$ is plotted versus $1/T_C$ for two types of films which differ by their thickness. For samples 1 and 2, the first three points are observed to be on a straight line. The following points draw another straight line which crosses the first one at finite temperature. The values of the slopes and of the ordinate axis intercepts determined by least squares are reproduced in Table 2. From Eq. (2) it can be seen that there is a compensation effect between the change of the activation energy $(C'' + B_2'')$ coming from the slope and frequency factors contained in the ordinate axis intercept. It must be remarked, as in the first series of experiments, that the variation of T_C contained in Eq. (2) does not affect significantly the aspect of our graphs in our range of measurement.

TABLE 2

Slopes and Ordinate Axis Intercepts Determined by the Least Squares Method. The Numbers Correspond to the Sequence of Measurements

	Ordinate axis intercept	Slope ($\times 10^3$)	$(C_2'' + B_2'') \times R$ (cal/mole) $\times 10^4$
• Sample 1 (130 Å)			
1-2-3	2.0	−3.8	1.52
4-5-6-7-8-9-10	4.4	−5.0	2.00
• Sample 2 (270 Å)			
1-2-3	0.3	−3.2	1.28
4-5-6-7-10-11-12-13-15-16	0.6	−5.2	2.08
•Sample 3 (270 Å)			
2-3-5	1.4	−3.7	1.48
4-6-7-8-9	4.6	−4.9	1.96

TABLE 3

Mean Crystallite Size in the Samples Determined by the Variance Method (*18*) after Annealing for 1 h (a) and 24 h (b) at 160°C in Pure CO at Atmospheric Pressure

Sample	Mean crystallite size (a) (Å)	Mean crystallite size (b) (Å)
1 (130 Å)	44	52
2 (270 Å)	51	64

c. *X-Ray Line-Broadening Measurements*

In thin films the main change with time and experiment conditions should be recrystallization. Thus, X-ray line-broadening ((111)reflection) analysis with the variance method (*18*) has been made in order to characterize the samples at the beginning and at the end of the experiments. The samples used were prepared at the same time as our small resistances. It has been found that the twin fault and deformation fault probabilities are very low. The line-broadening is entirely due to a size effect.

The mean crystallite size is given in Table 3 for two samples of different thickness (130 and 270 Å) after annealing in CO at 160°C for 1 h (corresponding to the beginning of the experiment) and for 24 h (nearly equivalent to the end of the measurements). Even if these values are not absolute, their different variations can be assumed to be significant. The difference of crystallite size between sample 1 and sample 2 (after the annealing for 24 h) appears rather clearly on the micrographs of Fig. 9.

DISCUSSION

The rise of T_C after each transition if no CO treatment is made could be correlated to the formation of "subsurface oxide" as

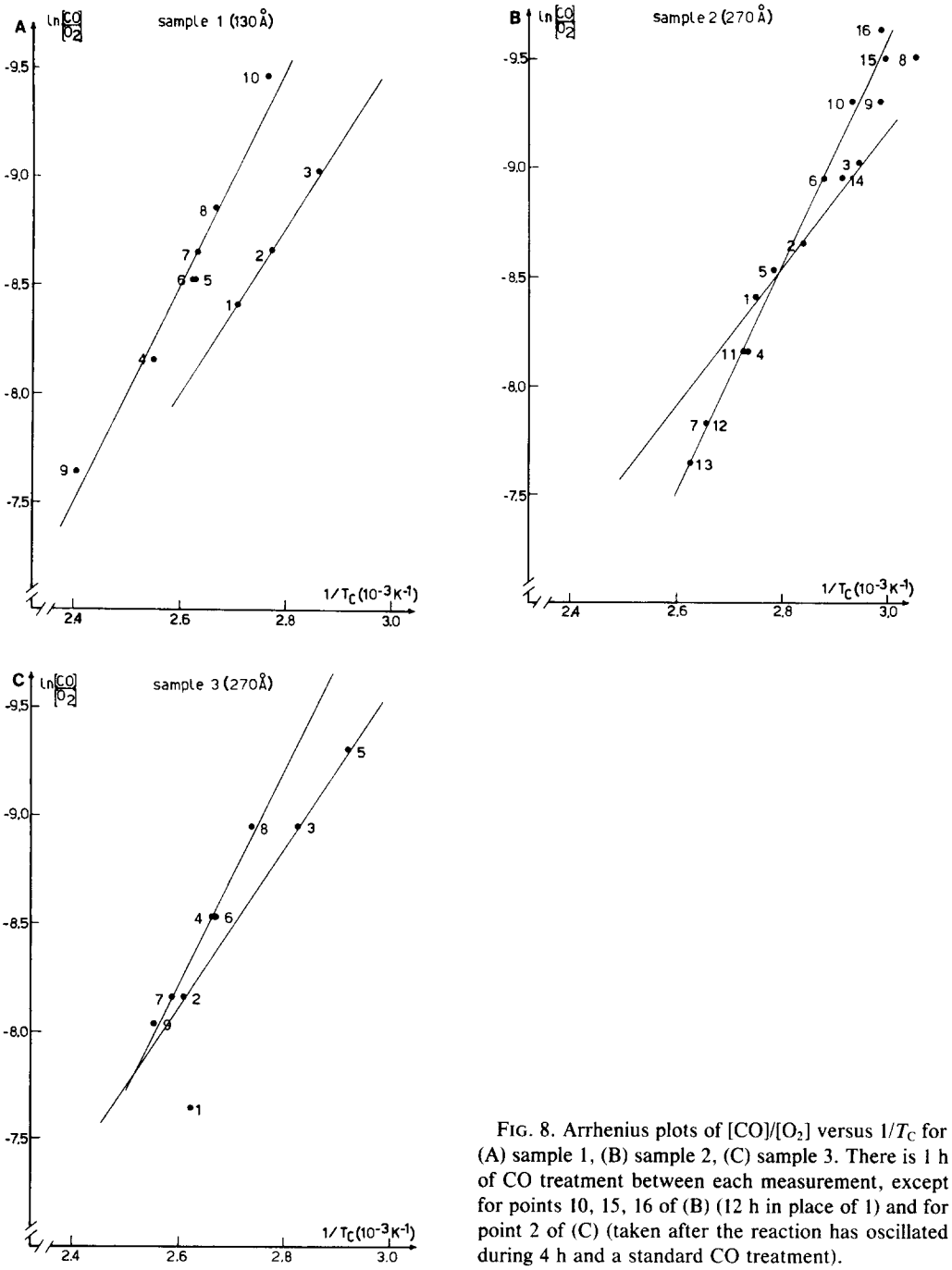

FIG. 8. Arrhenius plots of $[CO]/[O_2]$ versus $1/T_C$ for (A) sample 1, (B) sample 2, (C) sample 3. There is 1 h of CO treatment between each measurement, except for points 10, 15, 16 of (B) (12 h in place of 1) and for point 2 of (C) (taken after the reaction has oscillated during 4 h and a standard CO treatment).

described by numerous authors working on single crystals in U.H.V. (*11–14*). This oxygen "dissolution" would happen also during the transition from CO to oxygen coverage and would be the first step in the formation of a surface oxide and in turn the cause of its stability, as demonstrated by Salmeron *et al.* (*14*).

It could be argued that the temperature of the "subsurface" and surface oxide forma-

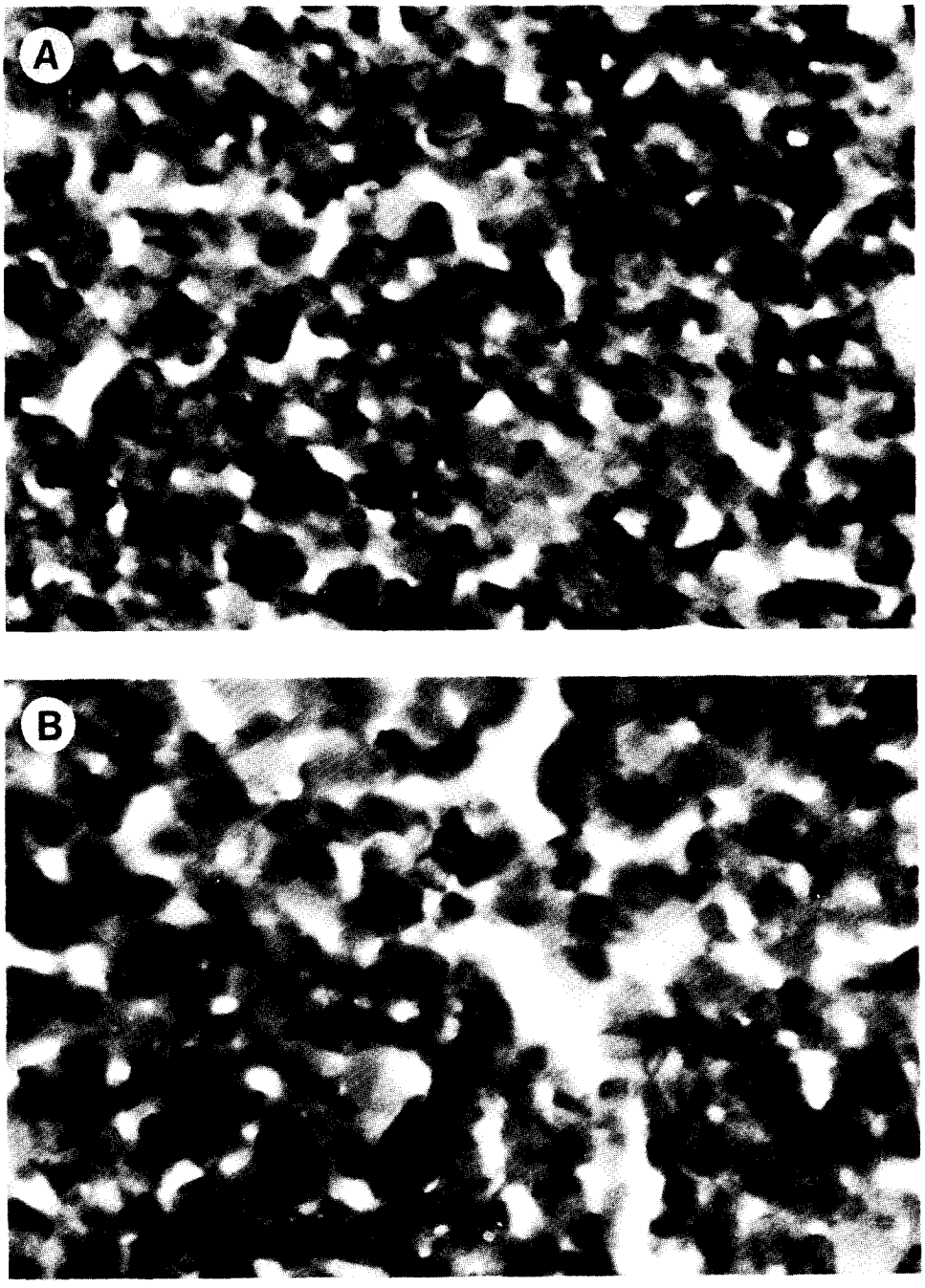

FIG. 9. Micrographs of (A) sample 1 and (B) sample 2 after an annealing of 24 h under CO at 160°C (magnification: 360,000).

tion is found to be higher in the U.H.V. experiments on single crystals than in our conditions. However, Sales *et al.* (*15*) have observed on polycrystalline platinum a real oxidation in a range of temperature as low as ours. On the other hand, Berry (*16*) has seen on platinum wire resistivity variations due to oxide formation between 350 and 500°C.

On the other hand, no obvious correla-

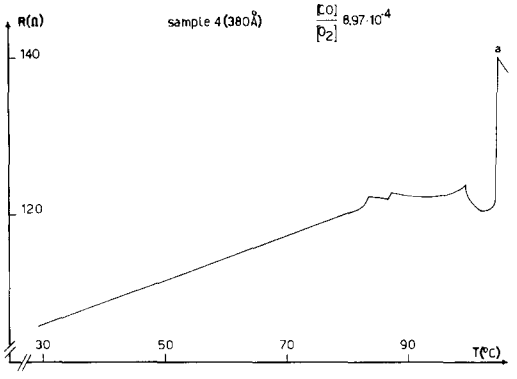

FIG. 10. Resistance behavior during heating in measurement mixture. Resistance jump due to the transition is observed at point a.

tion can be made between the mean crystallite size determined by X-ray diffraction and the characteristics of the straight lines given in Table 2.

However, the change undergone by the sample when the measurement is made at a temperature higher than about 90°C could be explained by a recrystallization. Indeed, the observation of a drop of resistivity at about 90°C, when a freshly decomposed sample is heated in the measurement mixture, supports this assertion (Fig. 10). Probably the crystallites implicated in this process are too small to influence the size measurement by X-ray diffraction and they recrystallize very slowly in pure CO since the sample is heated during 1 h at 160°C before the first measurement.

The absolute value of the slope is observed to be lower for the points taken at temperatures lower than about 90°C: this is at the beginning of the experiments (points 1, 2, 3 for the two first samples) or after a series of measurements at high temperature (points 8, 9, 14 of sample 2) for which it can be assumed that there is a large enough portion of small crystallites from where the reaction can be initiated and propagated on the rest of the surface (some measurements seem to prove that the transition propagates on the surface (*9*)). For T_C taken after a series of measurements at high temperature (for instance, points 8, 9, 14 of sample 2), it may be assumed that oxide islands which are formed on the surface during the transition when the surface becomes oxygen covered are reduced during CO treatment giving again small platinum crystallites which recrystallize only very slowly when they are in CO atmosphere. As a proof, an annealing as long as 12 h under CO is necessary to place points 10 and 15 (of sample 2) on the straight line of largest slope. This behavior is to be compared with the redispersion phenomena by oxidation–reduction cycles of supported platinum catalysts (*10, 19, 20*).

The main objection to our interpretation is a theoretical one. Indeed, there is no direct proof that our experimental conditions are such that Eq. (1) is valid. So it is necessary to consider again the DDN model (*4*) in the case of the LH mechanism (and $n = 2$). It must be noted that the LH mechanism is generally admitted to be predominant. Thus, the stationary conditions can be expressed as

$$\frac{dX}{dt} = B_1(1 - X - Y) - CXY = 0$$

$$\frac{dY}{dt} = B_2(1 - X - Y)^n - CXY = 0$$

with $n = 2$ in our case.

B_1, B_2, and C are the rate constants of, respectively, the carbon monoxide adsorption, the dissociative oxygen adsorption, and the surface reaction.

X and Y are the coverages in CO and atomic oxygen. These equations give:

$$X = \frac{B_2 - B_1}{2B_2}\left(1 \pm \sqrt{1 - \frac{4B_1^2B_2}{C(B_2 - B_1)^2}}\right)$$

$$Y = \frac{B_2 - B_1}{2B_2}\left(1 \pm \sqrt{1 - \frac{4B_1^2B_2}{C(B_2 - B_1)^2}}\right)$$

The condition leading to mixed adsorbates is

$$1 - \frac{4B_1^2B_2}{C(B_2 - B_1)^2} \geq 0.$$

In the particular case of the transition (at $T = T_C$)

$$\frac{4B_1^2B_2}{C(B_2 - B_1)^2} = 1.$$

With the conditions

$$0 \leq X \leq 1$$

$$0 \leq Y \leq 1$$

the equation obtained is

$$\frac{B_1'}{B_2'} = \frac{1}{e^{\left(\frac{B_2''-B_1''}{T_C}\right)}\left(1 + 2\sqrt{\frac{B_2'}{C'}}\, e^{-\left(\frac{B_2''-C''}{2T_C}\right)}\right)}$$

where

$$B_1' = \frac{\sigma_{CO}p_{CO}}{\sqrt{2\pi m_{CO}kT_C}}$$

and

$$B_2' = \frac{\sigma_{O_2}p_{O_2}}{\sqrt{2\pi m_{O_2}kT_C}}$$

B_1'' is the activation energy of carbon monoxide adsorption. It appears that the value of B_2' calculated by the relationship above and the value of C' given in the literature (*2, 25*) are of the same order of magnitude. Therefore, two limiting cases may be considered.

$$\text{(a)}\quad 2\sqrt{\frac{B_2}{C}} = 2\sqrt{\frac{B_2'}{C'}} \cdot e^{-\left(\frac{B_2''-C''}{2T_C}\right)} \gg 1$$

$$\text{(b)}\quad 2\sqrt{\frac{B_2}{C}} = 2\sqrt{\frac{B_2'}{C'}} \cdot e^{-\left(\frac{B_2''-C''}{2T_C}\right)} \ll 1$$

The thermal equation of Ref. (*4*) and the effects of diffusion of reactants need not be considered as long as the system is in the "inhibited" state (condition of our T_C measurements). Moreover, surface potential measurements have shown (*5*) that in the reaction conditions, just after the transition, the surface has a potential near the potential of the surface in pure oxygen. Since CO does not influence the surface potential, it must be concluded that the surface is nearly fully covered even in conditions of a very fast reaction. Therefore the consumption of reactants is always slower than their supply to the surface and it may be assumed that the first approximation (a) is applicable in our experimental conditions, which validates Eq. (1) ($B_2 > C$).

CONCLUSION

We have studied the transition between two stationary states of the carbon monoxide oxidation on platinum both at constant temperature and constant concentration.

At constant temperature it has been proved that the sense of variation of the CO concentration is important for the determination of the critical ratio [CO]*. The measurement depends on the sample geometry because of the heat dissipation and the diffusion of the reactants to the catalyst surface. The only way to determine [CO]* at constant temperature is thus in the decreasing [CO] sense.

At constant concentration we have tried to interpret the transition change (slope and ordinate axis intercept of the Arrhenius plot) as depending on the crystallographic morphology of the sample and on the oxygen dissolution in the sample. The dissolved oxygen can be removed by a CO treatment of 1 h at 160°C. At the same time oxide formed at the catalyst surface may be reduced and give smaller platinum crystallites.

The modulation of the transition by an oxidation–reduction treatment is a possible interpretation for the observed reaction oscillations in this system (*5, 17, 21–23*). Indeed, the opposite sense of change of transition in oxidizing and reducing coverage can be thought as the main cause of the oscillatory behavior.

This assumption was already made by Vayenas *et al.* (*24*) for the oscillating ethylene oxidation on platinum. However, the thermal effect at the surface which was first assumed (*4, 5*) and the diffusion of reactants to the surface cannot be neglected, as demonstrated here with experiments on two samples of different geometry.

It could be argued that there is no *direct* possibility of cross-checking our results. However, we aimed in this paper to describe a rather easy and original method to characterize thin film catalysts. Moreover, the values found for $C'' + B_2''$ are in agreement with the value of C'' and B_2'' given in the literature (*2, 25*).

It has been impossible, with the type of catalysts used, to control the change of the crystallite size distribution. Indeed, every transition can modify it. Measurements are now being made on epitaxial thin films for which it is possible to control crystallite size.

ACKNOWLEDGMENT

The authors thank M. Hecq for conducting X-ray diffraction measurements and X-ray line profile analysis.

REFERENCES

1. Engel, T., and Ertl, G., "Advances in Catalysis," Vol. 28, p. 1. Academic Press, New York, 1979.
2. Matsushima, T., Almy, D. B., and White, J. M., *Surf. Sci.* **67,** 89 (1977).
3. Golchet, A., and White, J. M., *J. Catal.* **53,** 266 (1978).
4. Dagonnier, R., Dumont, M., and Nuyts, J., *J. Catal.* **66,** 130 (1980).
5. Dauchot, J. P., and Van Cakenberghe, J., *Jpn. J. Appl. Phys. Suppl.* **2,** 533 (1974).
6. Hecq, M., Hecq, A., and Delrue, J. P., *J. Less-Common Met.* **64,** 25 (1979).
7. Mayadas, A. F., Shatzkes, M., *Phys. Rev. Ser. B* **1,** 1382 (1970).
8. Sondheimer, E. H., *Advan. Phys.* **1,** 1 (1952).
9. Dauchot, J. P., and Bertouille, T., *Vide, Couches Minces* Suppl. 201, vol. **1,** 548 (1980).
10. Ruckenstein, E., and Chu, Y. F., *J. Catal.* **59,** 109 (1979).
11. Niehus, H., and Comsa, G., *Surf. Sci.* **93,** L147 (1980).
12. Niehus, H., and Comsa, G., *Surf. Sci.* **102,** L14 (1981).
13. Gland, J. L., Sexton, B. A., and Fisher, G. B., *Surf. Sci.* **95,** 587 (1980).
14. Salmeron, M., Brewer, L., and Somorjai, G. A., *Surf. Sci.* **112,** 207 (1981).
15. Sales, B. C., Turner, J. E., and Maple, M. B., *Surf. Sci.* **112,** 272 (1981).
16. Berry, R. J., *Metrologia* **16,** 117 (1980).
17. Slin'ko, M. G., and Slin'ko, M. M., *Catal. Rev. Sci. Eng.* **17,** 119 (1978).
18. Hecq, M., Hecq, A., and Langford, J. I., *J. Appl. Phys.* **53** (1), 421 (1982).
19. Fiedorow, R. M. J., and Wanke, E., *J. Catal.* **43,** 34 (1976).
20. Chen, M., and Schmidt, L. D., *J. Catal.* **55,** 348 (1978).
21. Turner, J. E., Sales, B. C., and Maple, M. B., *Surf. Sci.* **103,** 54 (1981).
22. Wicke, E., Kummann, P., Keil, W., and Schiefler, J., *Ber. Bunsenges. Phys. Chem.* **84,** 315 (1980).
23. Sheintuch, M., and Schmitz, R. A., *Catal. Rev. Sci. Eng.* **15,** 107 (1977).
24. Vayenas, C. G., Georgakis, C., Michaels, J., and Tormo, J. *J. Catal.* **67,** 348 (1981).
25. Sales, B. C., Turner, J. E., and Maple, M. B., *Surf. Sci.* **114,** 381 (1982).